

## RESEARCH ARTICLE

10.1002/2017JD027058

## Key Points:

- CCN activity for aged aerosols is significantly underestimated, but it is overestimated for urban aerosols with large concentrations of primary particles
- The particle hygroscopicity parameter ( $\kappa$ ) was enhanced by between ~11% (polluted conditions) and 30% (clean days) due to the aging/coating effect
- CCN prediction exhibits very limited sensitivity to  $\kappa_{SOA}$ , implying a critical role of other factors in regulating CCN activity

## Correspondence to:

Z. Li,  
zli@atmos.umd.edu

## Citation:





Zhang, F., Wang, Y., Peng, J., Ren, J., Collins, D., Zhang, R., ... Li, Z. (2017). Uncertainty in predicting CCN activity of aged and primary aerosols. *Journal of Geophysical Research: Atmospheres*, 122. <https://doi.org/10.1002/2017JD027058>

Received 1 MAY 2017

Accepted 17 SEP 2017

Accepted article online 26 SEP 2017

## Uncertainty in Predicting CCN Activity of Aged and Primary Aerosols

Fang Zhang<sup>1,2</sup> , Yuying Wang<sup>1</sup>, Jianfei Peng<sup>3,4</sup>, Jingye Ren<sup>1</sup>, Don Collins<sup>3</sup> , Renyi Zhang<sup>3,4</sup>, Yele Sun<sup>5,6</sup> , Xin Yang<sup>1</sup> , and Zhanqing Li<sup>1,7</sup>

<sup>1</sup>State Key Laboratory of Earth Surface Processes and Resource Ecology, College of Global Change and Earth System Science, Beijing Normal University, Beijing, China, <sup>2</sup>Joint Center for Global Change Studies, Beijing, China, <sup>3</sup>Department of Atmospheric Sciences, Texas A&M University, College Station, TX, USA, <sup>4</sup>Department of Chemistry, Texas A&M University, College Station, TX, USA, <sup>5</sup>State Key Laboratory of Atmospheric Boundary Layer Physics and Atmospheric Chemistry, Institute of Atmospheric Physics, Chinese Academy of Sciences, Beijing, China, <sup>6</sup>Institute of Atmospheric Physics, University of Chinese Academy of Sciences, Beijing, China, <sup>7</sup>Earth System Science Interdisciplinary Center and Department of Atmospheric and Oceanic Science, University of Maryland, College Park, MD, USA

**Abstract** Understanding particle CCN activity in diverse atmospheres is crucial when evaluating aerosol indirect effects. Here aerosols measured at three sites in China were categorized as different types for attributing uncertainties in CCN prediction in terms of a comprehensive data set including size-resolved CCN activity, size-resolved hygroscopic growth factor, and chemical composition. We show that CCN activity for aged aerosols is unexpectedly underestimated ~22% at a supersaturation ( $S$ ) of 0.2% when using  $\kappa$ -Köhler theory with an assumption of an internal mixture with measured bulk composition that has typically resulted in an overestimate of the CCN activity in previous studies. We conclude that the underestimation stems from neglect of the effect of aging/coating on particle hygroscopicity, which is not considered properly in most current models. This effect enhanced the hygroscopicity parameter ( $\kappa$ ) by between ~11% (polluted conditions) and 30% (clean days), as indicated in diurnal cycles of  $\kappa$  based on measurements by different instruments. In the urban Beijing atmosphere heavily influenced by fresh emissions, the CCN activity was overestimated by 45% at  $S = 0.2\%$ , likely because of inaccurate assumptions of particle mixing state and because of variability of chemical composition over the particle size range. For both fresh and aged aerosols, CCN prediction exhibits very limited sensitivity to  $\kappa_{SOA}$ , implying a critical role of other factors like mixing of aerosol components within and between particles in regulating CCN activity. Our findings could help improving CCN parameterization in climate models.

## 1. Introduction

Owing to the significant spatial variations in aerosol physicochemical properties, the prediction of cloud condensation nuclei (CCN) number concentration ( $N_{CCN}$ ) in climate models is still fraught with large uncertainties, which leads to substantial biases in the estimates of aerosol indirect forcing (e.g., Sotiropoulou, Medina, & Nenes, 2006; Sotiropoulou et al., 2007; Wang, 2010). The largest uncertainties and errors in CCN prediction are found in heavily polluted regions (Sotiropoulou et al., 2007).

Köhler theory (Köhler, 1936) has been shown to adequately characterize the CCN activity of single-component and multicomponent aerosols in laboratory studies (e.g., Cruz & Pandis, 1997; Ma et al., 2013; Padro et al., 2007). Anthropogenic aerosols are more complex, and thus, application of Köhler theory-based models and parameterizations requires simplifying assumptions regarding particle composition and mixing state. To evaluate the uncertainty associated with these assumptions, a large number of studies aimed at quantifying how aerosol properties influence CCN activity in different environments have been performed (e.g., Chuang et al., 2000; Dusek et al., 2006; Gasparini et al., 2006; Chang et al., 2007; Wang et al., 2008, 2010; Bougiatioti et al., 2011; Padro et al., 2012; Bhattu & Tripathi, 2015; Deng et al., 2011; Zhang et al., 2014; Zhang, Li et al., 2016). The effects of composition, particle size, mixing state, and the aging process on CCN activity are still difficult to quantify. It is also not easy to accurately estimate CCN activity under different ambient conditions (Farmer et al., 2015; Seinfeld et al., 2016). Therefore, understanding how these different factors influence CCN activity in different environments is crucial in order to determine  $N_{CCN}$  accurately and, ultimately, to quantify aerosol indirect effects.

The use of aerosol optical measurements (e.g., aerosol optical depth, AOD) to estimate  $N_{\text{CCN}}$  is challenging because they are governed both by aerosol physicochemical properties and by environmental variables (Ghan et al., 2006; Andreae, 2009; Liu & Li, 2014). Field measurements of aerosols and CCN are vital for validating  $N_{\text{CCN}}$  retrieved from aerosol optical measurements as well as for improving CCN parameterizations in climate models. Different CCN parameterizations representing different atmospheric conditions are needed. However, concurrent and comprehensive measurement programs that include aerosol physicochemical properties and CCN activity from multiple sites are difficult to obtain due to the complexity of the instrumentation needed for measuring these parameters.

Using comprehensive data sets from three sites in China, we study the distinct CCN activity of a highly aged aerosol and of an aerosol in an environment strongly influenced by fresh aerosol emissions. We use the results to evaluate uncertainties in predicting  $N_{\text{CCN}}$  when applying a single hygroscopicity parameter,  $\kappa$ , retrieved from chemical composition. The sensitivity of  $N_{\text{CCN}}$  to the hygroscopicity of secondary organic aerosol (SOA) ( $\kappa_{\text{SOA}}$ ) is examined by assuming a series of different  $\kappa_{\text{SOA}}$  values. The goal of this work is to clarify which factors regulate CCN activity besides the well-known influences of chemical composition and particle size, and to improve the understanding of CCN prediction uncertainty for the aerosols typical of heavily polluted regions like northern China. We particularly focus on the effect of aging/coating on prediction of hygroscopicity and CCN number concentration.

## 2. Sites, Measurements, and Methodology

### 2.1. Sites

Field campaigns were conducted at three sites in China (Figure 1): Beijing (BJ: 39.97°N, 116.37°E, 49 m above sea level (asl)), Xianghe (XH: 39.80°N, 116.96°E, 35 m asl), and Xinzhou (XZ: 38.24°N, 112.43°E, 1,500 m asl). All sites are located on the North China Plain where rapid economic development has taken place over the past two decades and where the population density is high and the air is often polluted. Xianghe is located ~70 km to the southeast of BJ site, sitting between Beijing and Tianjin (a megacity in the region) and ~4 km west of the local town center. Located between two mountains (Taihang Mountain to the east and Lüliang Mountain to the west), the Xinzhou site is ~360 km to the southwest of BJ. The sampling site in Beijing is located at the Tower branch of the Chinese Academy of Sciences' Institute of Atmospheric Physics. It is subject to influences from local traffic and nearby cooking emissions (Sun et al., 2015). The Xianghe site is surrounded by agricultural land and densely occupied residences. The site experiences frequent pollution plumes, and pollutants of urban, rural, and mixed origins can be detected there. The Xinzhou site is also surrounded by agricultural land (e.g., corn fields), with relative less local pollution from motor vehicles and industrial activities. The site is at times downwind of Xinzhou City (with a population of 0.51 million) to the north and Taiyuan City, the capital of Shanxi Province, to the south. Because of its higher altitude, the site is often a receptor of aged aerosols transported to the area from other regions.

### 2.2. Measurements and Instrumentations

Size-resolved CCN measurements were conducted from 7 to 21 July 2013 at XH, 22 July to 26 August 2014 at XZ, and 8 November to 15 December 2014 and 28 August to 24 September 2015 at BJ. At the XH and XZ sites, a TSI Scanning Mobility Particle Sizer (SMPS) was combined with a Droplet Measurement Technologies Cloud Condensation Nuclei Counter (DMT-CCNc) (Lance et al., 2006) to measure size-resolved  $N_{\text{CCN}}$  and particle number size distributions (PSD) (Rose et al., 2008). The measured aerosol PSDs at the XH and XZ sites span the size range of 10–700 nm and 10–600 nm, respectively. At the BJ site, a custom high-flow scanning mobility particle sizer (SMPS; Wang & Flagan, 1990; Collins et al., 2002; Gasparini et al., 2004) combined with a DMT-CCNc was used. The aerosol PSD measured over a 3 min period at the BJ site spanned the size range of 15–600 nm. The aerosol inlet was equipped with a TSI Environmental Sampling System (Model 3031200), which consists of a sharp-cut  $\text{PM}_{10}$  (Particulate Matter with diameter < 1  $\mu\text{m}$ ) cyclone and a bundled Nafion dryer. The sampled particles were dried to  $\text{RH} < 30\%$  prior to introduction into the charge neutralizer and Differential Mobility Analyzer (DMA). At the XH and XZ sites the sample flow exiting the DMA was split into two parts: 0.3 liters per minute (Lpm) for the Condensation Particle Counter (CPC) and 0.5 Lpm for the CCNc. The DMA, controlled by TSI-AIM software, scanned one size distribution every 5 min. At the BJ site, the flow to the CCN counter was also 0.5 Lpm, but that to the CPC (a TSI 3760A) was 1.5 Lpm. The CCNc inlet  $\text{RH}$  was <30%. The supersaturation set points for each CCN measurement cycle were 0.07%, 0.1%, 0.2%, 0.4%,

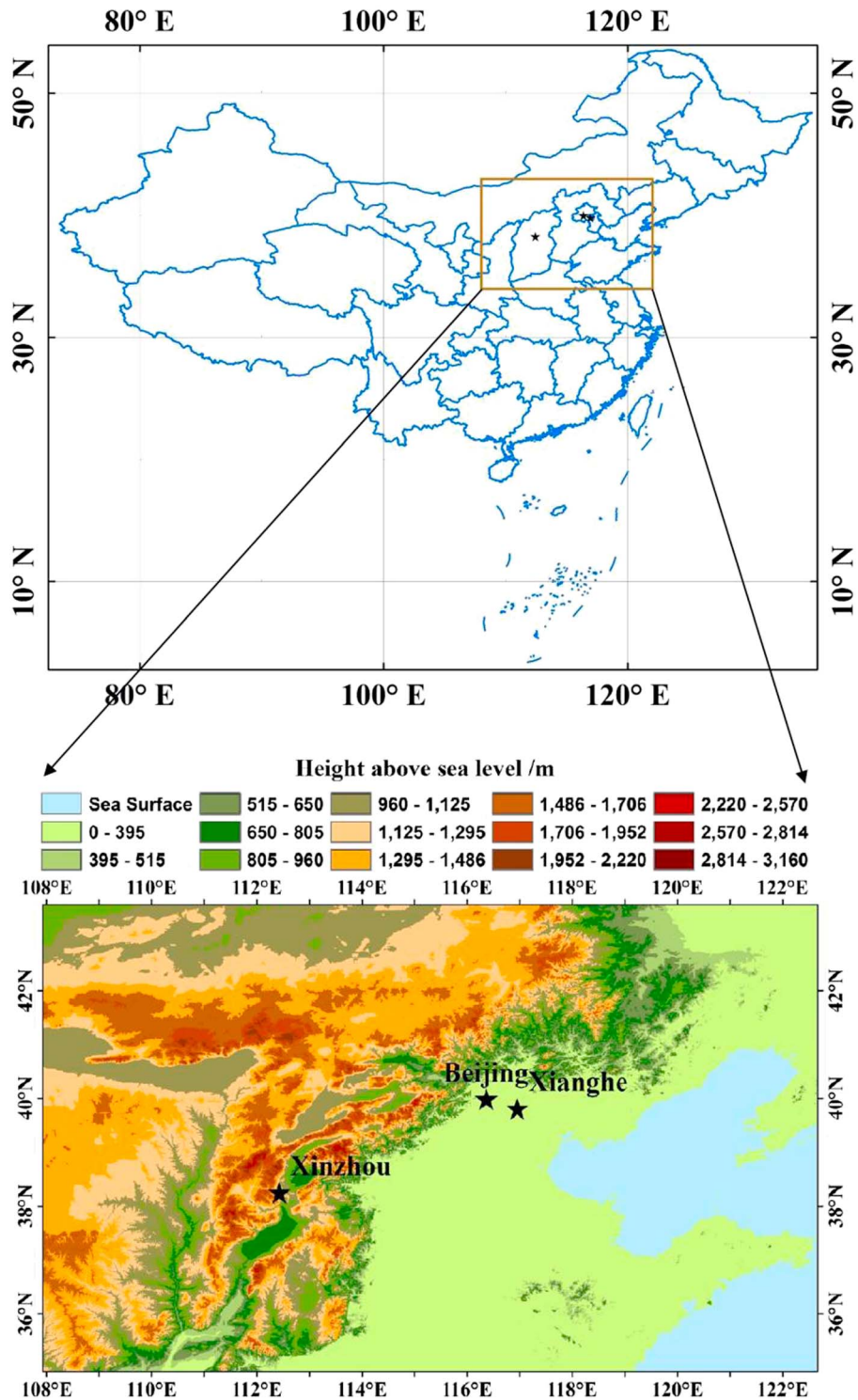


Figure 1. Map showing the locations of the study sites.

and 0.8%. The CCNc supersaturations were calibrated with ammonium sulfate before and after the field campaign, following the procedures outlined in Rose et al. (2008). The overall relative error ( $1\sigma$ ) was estimated to be  $<3.5\%$  of the set supersaturations. At the XZ and XH sites the completion of a full measurement cycle took 50 min (10 min for each supersaturation level). At the BJ site it took 70 min (14 min for each supersaturation level).

**Table 1**

Summary of the Mass Concentration ( $\mu\text{g}/\text{m}^3$ ) and Mass Fraction of Measured  $\text{PM}_{10}$  Aerosol Components and the Mean Atmospheric Temperatures and Relative Humidities (RH) at the Three Sites

Site	Sulfate (SO <sub>4</sub> %)	Nitrate (NO <sub>3</sub> %)	NH <sub>4</sub> (NH <sub>4</sub> %)	BC (BC%)	OA (OA%)	Temperature (°C)	Relative humidity
BJ	8.4 ± 9.7 (18.2 ± 8.3%)	7.3 ± 10.4 (15.3 ± 13.2%)	4.8 ± 6.0 (9.4 ± 5.4%)	2.2 ± 2.1 (6.3 ± 3.7%)	16.8 ± 7.0 (50.1 ± 12.1%)	21	66.4%
XH	12.8 ± 7.5 (18.8 ± 7.1%)	14.4 ± 9.9 (19.5 ± 6.8%)	8.8 ± 5.0 (12.6 ± 2.8%)	5.4 ± 3.4 (7.9 ± 3.1%)	27.5 ± 13.9 (35.8 ± 6.1%)	24	72.3%
XZ	11.5 ± 8.3 (31.0 ± 8.3%)	5.1 ± 4.3 (13.3 ± 6.5%)	4.2 ± 2.8 (11.2 ± 2.9%)	2.4 ± 1.6 (7.4 ± 4.6%)	13.7 ± 5.0 (35.5 ± 5.2%)	22	72.3%

Aerosol hygroscopic growth factor ( $gf$ ) was measured at the sites using Hygroscopic Tandem Differential Mobility Analyzers (HTDMA). The HTDMA systems consist of four main parts:

1. A Nafion dryer (model PD-70 T-24ss, Perma Pure Inc., USA) and bipolar neutralizer (Kr85, TSI Inc.). The Nafion dryer ensured that the RH of the sample flow was below 20% over the study period, and the bipolar neutralizer was used to produce a steady state particle charge distribution (Wiedensohler, 1988).

2. The first differential mobility analyzer (DMA1, TSI Inc. or fabricated DMA) (Wang et al., 2017; Zhang, Ma et al., 2016; Gasparini et al., 2004) was used to select quasi-monodisperse particles of a selected diameter by applying a fixed high voltage.

3. A Nafion humidifier (model PD-70T-24ss, Perma Pure Inc., USA) was used to humidify the aerosol flow from DMA1 to a defined RH. The RH was set to 90%, 87%, and 85% at BJ, XH, and XZ, respectively.

4. The second DMA (DMA2, same model as DMA1) and a CPC (TSI Inc.) were used together to measure the number size distribution of the humidified particles. The measurement uncertainty of the HTDMA mainly depends on the accuracy of the measured RH in DMA2 and the possible sizing bias between the two DMAs (Massling et al., 2007). The RH was calibrated during the campaigns by measuring the growth factor of pure ammonium sulfate particles of 100 nm dry diameter. The estimated uncertainty in RH was  $\pm 1\%$ , resulting in a relative uncertainty of around 2.5% for the  $gf$  of ammonium sulfate particles at 90% RH (Massling et al., 2003). The offset in sizing between the two DMAs was determined by measuring the apparent  $gf$  of Polystyrene Latex spheres (PSL, ThermoScientific, Duke Standards) with no humidification between the DMAs. The offset in sizing was observed to be less than 3%, which is within the expected range for such systems (Wiedensohler et al., 2012). More detailed information about the systems used at the BJ, XH, and XZ sites can be found in Tan et al. (2013) or Wang et al. (2017), Zhang, Ma et al. (2016), and Gasparini et al. (2004), respectively.

Submicron nonrefractory aerosol species including organics, sulfate, nitrate, ammonium, and chloride were measured using an Aerosol Chemical Speciation Monitor (ACSM; Sun et al., 2012; Wang et al., 2016). Positive matrix factorization (PMF) with the PMF2.exe (v4.2) algorithm (Paatero & Tapper, 1994) was used to analyze the ACSM organic spectral matrices following the procedures reported in Ulbrich et al. (2009). Use of PMF provided the mass fractions of primary organic aerosol (POA) and secondary organic aerosol (SOA). More detailed descriptions of the operation and calibration of the ACSM are not addressed here but can be found in Ng et al. (2011). In addition to the ACSM, the black carbon (BC) concentration in  $\text{PM}_{2.5}$  was measured with a time resolution of 5 min by a BC analyzer (Aethalometer, Model AE22, Magee Scientific Corporation). The campaign-averaged mass concentrations and mass fractions of the measured aerosol components are summarized in Table 1.

### 2.3. Derivation of the Particle Hygroscopicity Parameter, $\kappa$

Here we derive  $\kappa$  using  $\kappa$ -Köhler theory (Petters & Kreidenweis, 2007) using either CCN activity data ( $\kappa_{\text{CCN}}$ ) or HTDMA-determined  $gf$  ( $\kappa_{\text{HTDMA}}$ ). For  $\kappa_{\text{CCN}} > 0.1$  the following approximate expressions can be used (Petters & Kreidenweis, 2007):

$$\kappa_{\text{CCN}} = \frac{4A^3}{27D_p^3 S_c^2}, \quad (1)$$

$$A = \frac{4\sigma_w M_w}{RT\rho_w}, \quad (2)$$

where  $S_c$  is the particle critical supersaturation and is the  $S$  at which the activation ratio (AR) reaches 50% of  $E$ . It is derived using the approach described by Rose et al. (2008) and Mei et al. (2013).  $D_p$  is the particle dry

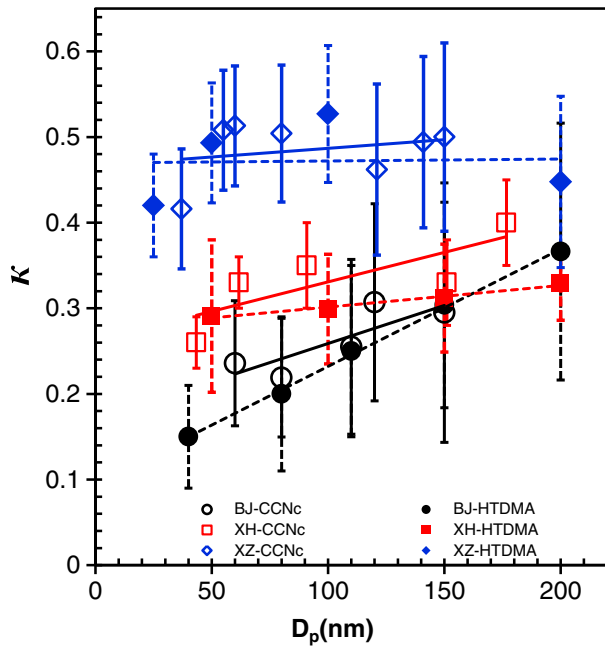


**Figure 2.** The dependence of  $\kappa$  on  $D_p$  at three sites. The  $\kappa$  values are retrieved from both size-resolved CCNc and HTDMA measurements. The  $\kappa_{\text{HTDMA}}$  at XH is from Zhang, Ma et al. (2016). The solid and open symbols represent the  $\kappa_{\text{HTDMA}}$  and  $\kappa_{\text{CCN}}$  respectively, and the circles, squares, and diamonds represent the values observed at BJ, XH, and XZ sites, respectively. The error bars represent  $\pm 1\sigma$ .

from previous laboratory experiments (Petters & Kreidenweis, 2007). The following linear function derived by Mei et al. (2013) was used to estimate  $\kappa_{\text{org}}$  in our study:  $\kappa_{\text{org}} = 2.10 \times f_{44} - 0.11$ . The particle hygroscopicity is thus the volume average of the three participating species. Species volume fractions were derived from mass concentrations and densities of the participating species. The densities of  $(\text{NH}_4)_2\text{SO}_4$  and  $\text{NH}_4\text{NO}_3$  are  $1,770 \text{ kg m}^{-3}$  and  $1,720 \text{ kg m}^{-3}$ , respectively. The density of organics was assumed to be  $1,200 \text{ kg m}^{-3}$  (Turpin et al., 2001). More detailed descriptions of the method to retrieve  $\kappa_{\text{chem}}$  can be found in Zhang et al. (2014). A quick comparison between  $gf$ -derived and CCN-derived  $\kappa$  values as a function of particle size at the three sites is shown in Figure 2. For particle diameter ranging from 40 to 200 nm the differences between  $gf$ -derived and CCN-derived  $\kappa$  values are less than 20% for all sites. The CCN-derived  $\kappa$  at the three different sites was slightly higher than that derived from the HTDMA data. Similar disparities have been reported by others (e.g., Cerully et al., 2011; Good et al., 2010; Irwin et al., 2010; Wex et al., 2009; Wu et al., 2013). Possible explanations include nonideality effects in the solution droplets, surface tension reduction due to surface active substances, and the presence of slightly soluble substances that dissolve at RH higher than that maintained in the HTDMA (Wex et al., 2009). Both the  $\kappa_{\text{CCN}}$  and  $\kappa_{\text{HTDMA}}$  observed at XZ are much higher than that observed at BJ and XH, and also higher than reported values at most other continental sites in China (e.g., Jiang et al., 2016; Liu et al., 2011; Ye et al., 2013).

#### 2.4. Identification of Aerosol Type From CCNc and HTDMA Measurements

We fit the size-resolved CCN curves using a lognormal function with the maximum activated fraction ( $E$ ) and critical supersaturation ( $S_c$ ) among the fitting parameters (Mei et al., 2013). For each set of measurements, the function form that yielded the best fit (i.e., the smallest least squares residual) was employed for deriving the size-selected AR curves. The AR typically increased with increasing  $S$  until reaching  $E$ . The difference between 1.0 and  $E$  represents the number fraction of nonhygroscopic primary particles that cannot serve as CCN for typical atmospheric supersaturations, which normally range from 0.1 to 0.7% in cumulus clouds (Pruppacher & Klett, 2000). The characteristic  $S_c$  of a size-resolved population of particles is the  $S$  at which the AR reaches 50% of  $E$ . The slope of the AR with respect to  $S$  near  $S_c$  provides information about the heterogeneity of the composition for the size-selected particles.

diameter,  $M_w$  is the molecular weight of water,  $\sigma_w$  is the surface tension of pure water,  $\rho_w$  is the density of water,  $R$  is the gas constant, and  $T$  is the absolute temperature. Note that values derived from CCN measurement data through Köhler model calculations that assume the surface tension of pure water have to be regarded as “effective hygroscopicity parameters” that account not only for the reduction of water activity by the solute (“effective Raoult parameters”) but also for surface tension effects (Petters & Kreidenweis, 2007).  $\kappa_{\text{HTDMA}}$  can be calculated from the following expression:

$$\frac{\text{RH}}{\exp\left(\frac{A}{gfD_p}\right)} = \frac{gf^3 - 1}{gf^3 - (1 - \kappa)}, \quad (3)$$

where RH is expressed as a fraction.  $A$  is the same as in equation (2).

As proposed by Petters and Kreidenweis (2007),  $\kappa_{\text{chem}}$  is calculated using a simple mixing rule based on chemical volume fractions for an assumed internal mixture:

$$\kappa_{\text{chem}} = \sum_i \varepsilon_i \kappa_i, \quad (4)$$

where  $\kappa_i$  and  $\varepsilon_i$  are the hygroscopicity parameter and volume fraction, respectively, for the individual (dry) components in the mixture and  $i$  is the number of components in the mixture. For this analysis the bulk composition measured by the ACSM is used to calculate  $\kappa_{\text{chem}}$ . The aerosol components measured by the ACSM mainly consisted of organics,  $(\text{NH}_4)_2\text{SO}_4$ , and  $\text{NH}_4\text{NO}_3$  (Zhang et al., 2014; Zhang, Li et al., 2016). The values of  $\kappa$  are 0.67 and 0.61 for  $(\text{NH}_4)_2\text{SO}_4$  and  $\text{NH}_4\text{NO}_3$ , respectively, which are derived

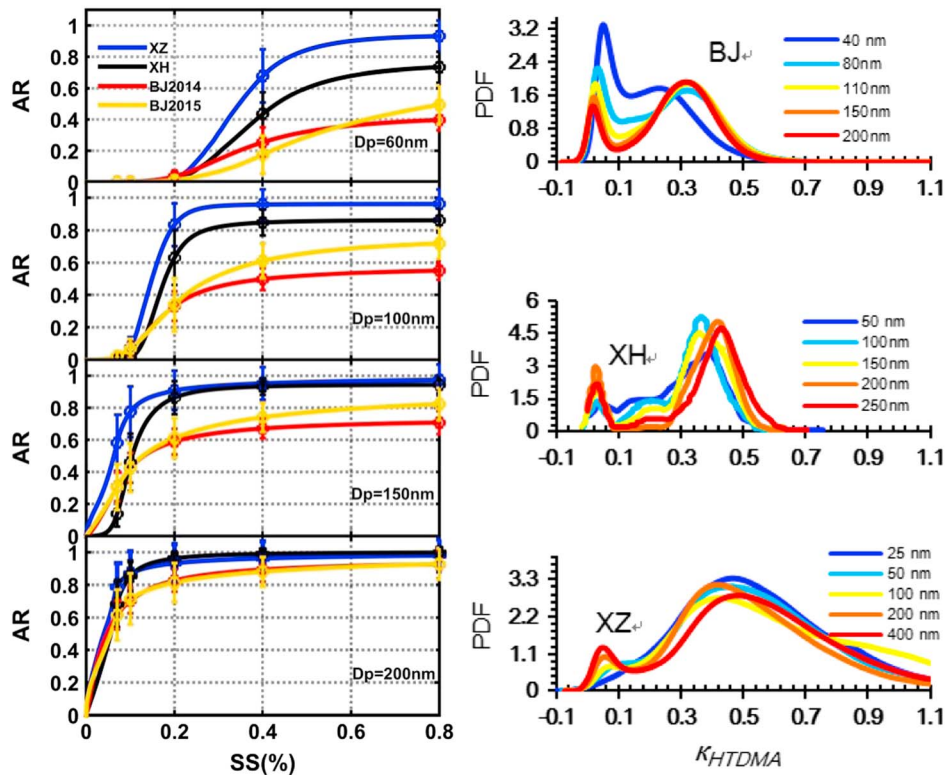


**Figure 3.** CCN activation ratios (AR) as a function of (left column) supersaturation and (right column) size-resolved mean probability distribution functions (PDFs) of the HTDMA-retrieved hygroscopicity parameter ( $\kappa_{HTDMA}$ ) at the three sites: Beijing (BJ), Xianghe (XH), and Xinzhou (XZ). The PDFs of  $\kappa_{HTDMA}$  at the XH site are from Zhang, Ma et al. (2016).

The lognormal function fits of the size-resolved CCN activity (presented in the middle of Figure 3) show differences between the three locations. Maximum CCN activation ratios at BJ in both 2014 and 2015 were significantly below 1 at a supersaturation of 0.8%, which suggests a large contribution of externally mixed low hygroscopicity or hydrophobic particles, which is also indicated by the HTDMA measurements shown in Figure 3 (right column). At BJ, even at 150 nm dry  $D_p$  a significant fraction of the particles did not activate at  $S = 0.8\%$ . The mean  $\kappa_{HTDMA}$  probability distribution functions (PDFs) shown in Figure 3 show high-amplitude peaks at  $\kappa_{HTDMA} < 0.05$  at BJ for particles with  $D_p$  ranging from 40 to 200 nm, reflecting the significant impact of local primary emissions (e.g., vehicle emissions and cooking sources) (Sun et al., 2015; Vu et al., 2017). The PDFs at each site have tails that extend to  $\kappa < 0$ , though the impact is  $< 0.02\%$  and deemed negligible. The comparatively shallow slopes around  $S_c$  at the BJ site indicate that particle composition there was more heterogeneous than at the XH and XZ sites, particularly for particles with  $D_p < 100$  nm. The steeper slopes for the data from the XZ site suggest greater uniformity in particle hygroscopicity, which is expected with an aged and internally mixed aerosol. The corresponding PDF of  $\kappa_{HTDMA}$  possesses a single dominant peak. The XH site is influenced by a mixture of local primary emissions and aged particles and consequently has higher  $\kappa$  values than at the BJ site but lower  $\kappa$  values than at the XZ site (also shown in Figure 2).

The mass concentration of organics accounted for about 50.1%, 35.8%, and 35.5% of the total  $PM_{10}$  at the BJ, XH, and XZ sites, respectively (Table 1). Combining the analyses of the size-resolved CCN AR curves, the PDFs of  $\kappa_{HTDMA}$ , and the chemical composition information, the aerosol characteristics of the BJ, XH, and XZ sites during the observation periods were categorized as primary, transitional, and aged, respectively.

### 3. Results and Discussion

#### 3.1. Critical Supersaturation Dependence on $D_p$

The study-average size dependence of  $S_c$  for the three sites is presented in Figure 4. For comparison, the  $S_c$  of particles composed of pure ammonium sulfate, fresh soot, and pinic acid (Ma et al., 2013) is also shown. For

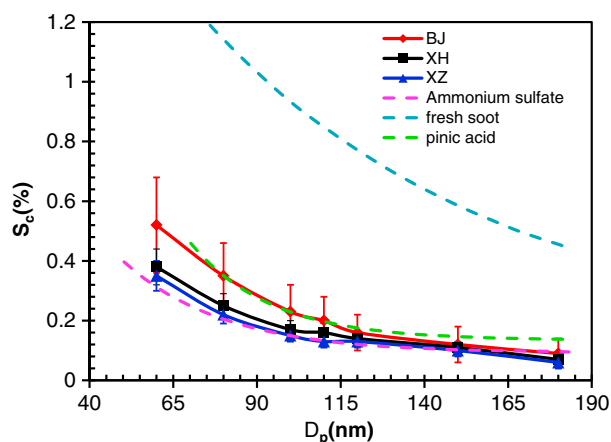


**Figure 4.** Critical supersaturation ( $S_c$ ) as a function of particle diameter ( $D_p$ ) at BJ (red line), XH (black line), and XZ (blue line). Lab measurements (Ma et al., 2013) for fresh soot (light blue dashed line), pure ammonium sulfate ( $\kappa = 0.61$ , pink dashed line) and pinic acid ( $\kappa = 0.248$ , green dashed line) are included for comparison.

both ambient particles and pure compounds, an increase in particle size generally causes a reduction in  $S_c$ , because of a reduced Kelvin effect and an increased Raoult effect (Koehler, 1936). The effect of the chemical composition and/or mixing state on  $S_c$  is illustrated by the different trends of  $S_c$  among different sites. Aerosols composed of aged and internally mixed particles usually require a lower  $S$  to activate than do freshly primary particles. Among the three sites, the more aged particle characteristics of XZ had the lowest  $S_c(D_p)$ . The magnitude of the differences between the  $S_c$  at the different sites increased with decreasing particle size. For example, the mean  $S_c$  is 0.34% at XZ and 0.52% at BJ for  $D_p = 60$  nm, while they are in close agreement for particles with  $D_p > 150$  nm. This largely reflects the significant difference in hygroscopicity of the smaller particles coupled with the similarity in hygroscopicity of the larger particles that are generally aged and coated.

Overall, compared with laboratory experiment results for pure compounds, the CCN activity recorded at the XZ site is similar to that of pure ammonium sulfate ( $\kappa = 0.61$ ) (Clegg et al., 1998). The  $S_c$  observed at the BJ site is comparable to that of pure organic acids such as pinic acid ( $\kappa = 0.248$ ) and to that of SOA particles (Prenni et al., 2007).

The size-dependent  $S_c$  at the XH site was higher than at XZ but lower than at BJ. However, the calculated hygroscopicity parameter derived from the chemical composition,  $\kappa_{chem}$ , at the XZ site ( $\sim 0.41$ ) is much lower than that of pure ammonium sulfate, while  $\kappa_{chem}$  at the BJ site ( $\sim 0.32$ ) is much higher than that of pure pinic acid. This implies that  $\kappa_{chem}$  may underestimate the CCN activity at XZ and overestimate it at BJ.

### 3.2. Comparison of Mean $\kappa_{CCNC}$ , $\kappa_{HTDMA}$ , and $\kappa_{chem}$

The mean  $\kappa_{chem}$  is compared with that derived from the CCNC ( $\kappa_{CCNC}$ ) and HTDMA ( $\kappa_{HTDMA}$ ) measurements in Figure 5. Here  $\kappa_{chem}$  is calculated from the bulk  $PM_{10}$  composition, whereas  $\kappa_{CCNC}$  and  $\kappa_{HTDMA}$  are arithmetic

means based on measurements of particles with diameters between about 40 and 200 nm. Because of the dependence of chemical composition on particle size, bulk  $\kappa_{chem}$  may overestimate the particle hygroscopicity at BJ because the ACSM measurements show aerosol volume was dominated by particles with  $D_p > 60$  nm, though Wu et al. (2016) demonstrated that such a dependence of  $D_p$  on chemical composition is negligible in urban areas. As is shown in Figure 5 the mean  $\kappa_{CCNC}$  and  $\kappa_{HTDMA}$  at BJ are much lower than  $\kappa_{chem}$  derived from the ACSM measurements. At the XZ site where the aerosol is more aged and chemically homogeneous, the dependence of composition on particle size is expected to be negligible. The  $\kappa_{CCNC}$  and  $\kappa_{HTDMA}$  at XZ show no trend with  $D_p$  (as shown in Figure 3).

The  $\kappa_{chem}$  at XZ is much lower ( $0.41 \pm 0.06$ ) than  $\kappa_{CCNC}$  ( $0.48 \pm 0.07$ ) and  $\kappa_{HTDMA}$  ( $0.47 \pm 0.03$ ), with differences of 18.3%  $\pm$  5.0% between  $\kappa_{chem}$  and  $\kappa_{CCNC}$  and 15.1%  $\pm$  3.6% between  $\kappa_{chem}$  and  $\kappa_{HTDMA}$ . The lower  $\kappa_{chem}$  would yield a larger critical diameter or higher  $S_c$ , and thus a lower CCN and cloud droplet concentration, which will in turn lead to uncertainty in evaluating the associated aerosol indirect effects on clouds and climate. On the contrary, calculated  $\kappa_{chem}$  at the BJ site is  $0.32 \pm 0.11$ , which is considerably higher than  $\kappa_{CCNC}$  ( $0.26 \pm 0.04$ ) and  $\kappa_{HTDMA}$  ( $0.25 \pm 0.08$ ), with corresponding overall differences of 24.6%  $\pm$  7.7% between  $\kappa_{chem}$  and  $\kappa_{CCNC}$  and 29.6%  $\pm$  15.4% between  $\kappa_{chem}$  and  $\kappa_{HTDMA}$ . The higher  $\kappa_{chem}$  would accordingly result in a smaller critical diameter or lower  $S_c$ , and consequently higher estimated CCN and cloud droplet concentration.

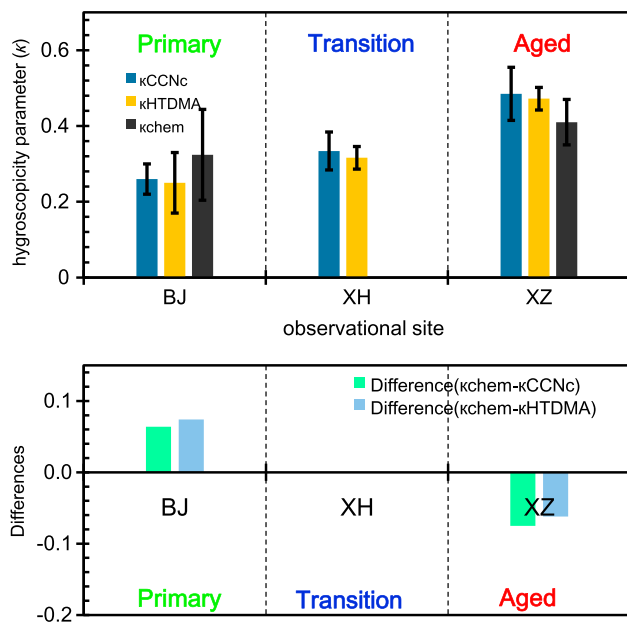


**Figure 5.** Mean  $\kappa$  retrieved from (top) CCN, HTDMA, and ACSM measurements and differences between (bottom)  $\kappa_{chem}$  and  $\kappa_{CCNC}$  and  $\kappa_{HTDMA}$  at the three sites. For comparison,  $\kappa_{HTDMA}$  at BJ is calculated only using the  $\kappa$  values for  $D_p > 100$  nm due to the strong dependence of  $\kappa$  on  $D_p$  at the site. No ACSM was available for chemical composition measurements at the XH site, though an intermediate  $\kappa_{chem}$  value is expected there.

Although the ACSM-based  $\kappa$  may overestimate particle hygroscopicity because of its sensitivity to larger particles, the mean  $\kappa_{\text{chem}}$  at XZ is much lower than  $\kappa_{\text{CCNc}}$  and  $\kappa_{\text{HTDMA}}$ . Indeed, as shown in Figure 3,  $\kappa_{\text{CCNc}}$  and  $\kappa_{\text{HTDMA}}$  show no apparent size dependence because upwind processing of the aerosol results in uniform composition over the full size range. One explanation for the lower  $\kappa_{\text{chem}}$  at XZ is uncertainty in the hygroscopicity of organic aerosols ( $\kappa_{\text{org}}$ ) because it is assumed to be a simple linear function of  $f_{44}$  (Mei et al., 2013). Because the coefficients in the linear function ( $\kappa_{\text{org}} = 2.10 \times f_{44} - 0.11$ ) are based on measurements in different regions, they may not be applicable for the aerosols sampled during this study. However, increasing  $\kappa_{\text{SOA}}$  to an upper limit value of 0.3 (Jimenez et al., 2009; Petters & Kreidenweis, 2007; Petters et al., 2016) increases  $\kappa_{\text{chem}}$  only to 0.43, which is still lower than  $\kappa_{\text{CCNc}}$  and  $\kappa_{\text{HTDMA}}$ . An underestimate of  $\kappa_{\text{org}}$  thus cannot fully explain the low  $\kappa_{\text{chem}}$  at XZ. Another cause may be the particle aging/coating process, for example, condensation of secondary aerosol (sulfate and nitrate) on preexisting particles. The resulting particle hygroscopicity may depend more on the coating layer than on the original particle composition (Ma et al., 2013). In that case, for example, preexisting primary particles like hydrophobic soot that are coated by hygroscopic substances will not strongly influence the overall particle hygroscopicity and CCN activity. This effect will also be discussed in section 3.4.

For the aerosol sampled at the BJ site where primary particles make up a significant fraction of the overall concentration the hygroscopicity is overestimated by the bulk  $\kappa_{\text{chem}}$  model. One likely cause of this bias is that ACSM measurements indicate that aerosol volume was dominated by particles with  $D_p > 60$  nm, and the hygroscopicity for particles  $< 60$  nm is much lower than that of the larger particles. Additionally, the distribution of hygroscopicity in an external mixture (McFiggans et al., 2006; Figure 3) such as that commonly found in urban areas such as Beijing is not captured in the calculations and may have contributed to the bias. An inaccurate assumption on particle mixing state could result in either an overestimate or an underestimate of the  $\kappa$  and thus lead to uncertainties in predicting  $N_{\text{CCN}}$  (Padro et al., 2012) and cloud droplet concentration. It may also be that the  $\kappa_{\text{org}}$  used is higher than it should be, though to force  $\kappa_{\text{chem}}$  to match  $\kappa_{\text{CCNc}}$  requires the unreasonable assumption that the organic component is completely nonhygroscopic with  $\kappa_{\text{org}} = 0$ .

### 3.3. Prediction of CCN Number Concentrations

To further assess the potential effect of  $\kappa_{\text{chem}}$  on evaluating CCN activity of the distinct types of aerosols observed at XZ and BJ,  $N_{\text{CCN}}$  is estimated.

The critical dry diameter ( $D_{\text{crit}}$ ) was calculated to predict the total CCN number concentration ( $N_{\text{CCN\_Predicted}}$ ) based on  $\kappa$ -Köhler theory (Petters & Kreidenweis, 2007), where the  $D_{\text{crit}}$  of a particle population with properties ( $S_c$ ,  $\kappa_{\text{chem}}$ ) corresponds to the minimum  $D$  needed for activation. The  $N_{\text{CCN\_Predicted}}$  was then obtained from the step-wise integration of the particle number size distribution from  $D_{\text{crit}}$  to 600 nm for the data sets collected at the XZ and BJ sites. The sensitivity of  $N_{\text{CCN}}$  to the hygroscopicity of SOA ( $\kappa_{\text{SOA}}$ ) is also examined by assuming a series of  $\kappa_{\text{SOA}}$  values (0.07, 0.1, 0.2, and 0.3). The  $\kappa$  of primary organic aerosol  $\kappa_{\text{POA}}$  is assumed to be 0 because POA is thought to be hydrocarbon like (Zhang et al., 2004) and aliphatic in nature and, in general, those types of compounds have not been found to be CCN active in laboratory experiments (e.g., Pradeep et al., 2003) and field measurements (Cubison et al., 2008).

The accuracy of the prediction of  $N_{\text{CCN}}$  using bulk  $\kappa_{\text{chem}}$  is dependent upon  $S$ , with typically underestimated concentrations at low  $S$  but always overestimated concentrations at high  $S$  (e.g., Juranyi et al., 2010). This reflects the observed size dependence of hygroscopicity, with the mean bulk  $\kappa_{\text{chem}}$  derived from  $\text{PM}_{10}$  usually higher than the hygroscopicity of smaller particles (corresponding to the critical diameter at high  $S$ ) but lower than that of larger particles (corresponding to the critical diameter at low  $S$ ). Normally, the mean bulk  $\kappa_{\text{chem}}$  is closest to the hygroscopicity of particles with  $D_p$  of 100–150 nm, corresponding to  $S$  of 0.1–0.2%. Such an effect can be neglected at XZ because of the weak size dependence of  $\kappa$  but is expected to be large at BJ due to the strong size dependence there. The analysis below is thus limited to the results for  $S = 0.2\%$  to focus on the effect of aging/coating without the complicating dependence on  $S$ .

The sensitivity of  $N_{\text{CCN\_predicted}}$  to the hygroscopicity of SOA ( $\kappa_{\text{SOA}}$ ) is shown in Figures 6a and 6b for calculations assuming the particles are internally mixed with a size-independent composition (BK-INT scheme).

Our results show that for the XZ site  $N_{\text{CCN}}$  at  $S = 0.2\%$  was underestimated by ~22% when calculated from the  $f_{44}$ -derived  $\kappa_{\text{chem}}$ . Based on the differences between  $\kappa_{\text{chem}}$  and  $\kappa_{\text{CCNc}}$  or  $\kappa_{\text{HTDMA}}$  discussed in section 3.2 and



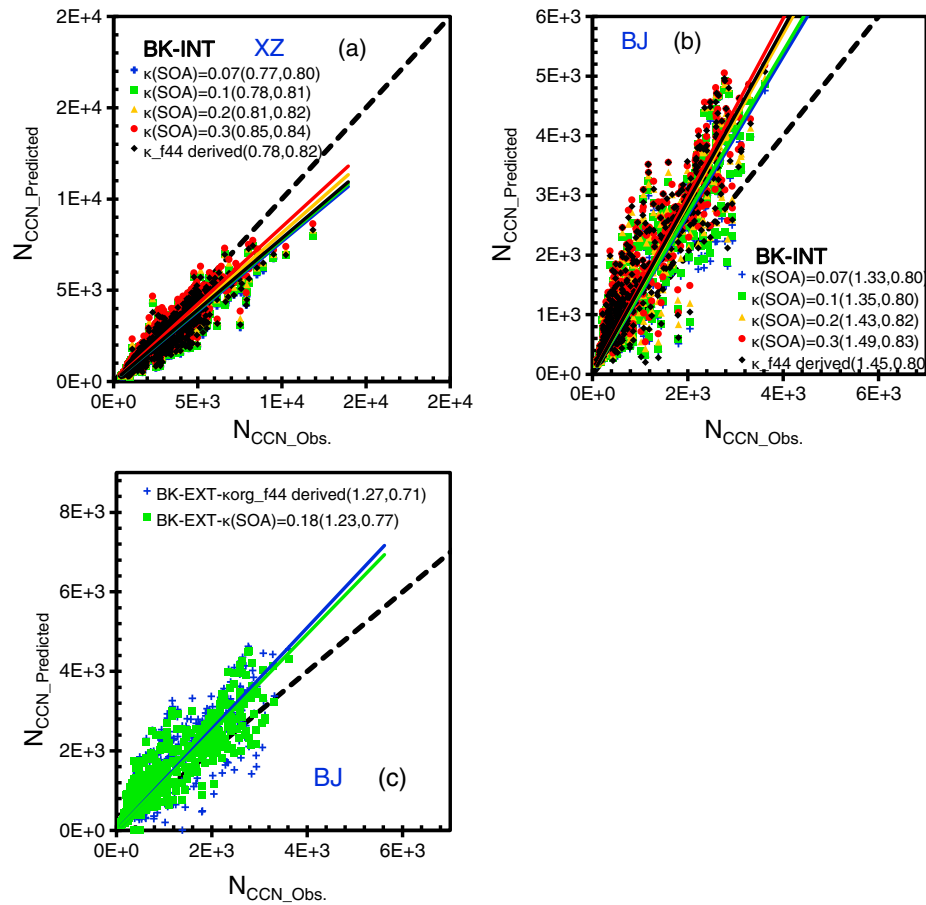


**Figure 6.** Observed and predicted  $N_{CCN}$  ( $S = 0.2\%$ ) at the XZ and BJ sites. (a) XZ results using an internally mixed scheme (BK-INT); (b) BJ results using the Bulk-INT scheme; (c) BJ results using the BK-EXT scheme (assuming particles are externally mixed but with a size-independent composition). Here the sensitivity of CCN number concentrations to the hygroscopicity of SOA ( $\kappa_{SOA}$ ) in the BK-INT scheme is examined by assuming a series of  $\kappa_{SOA}$  values (0.07, 0.1, 0.2, and 0.3), represented by different colors and symbols. The green solid squares in Figure 6c are results obtained by assuming  $\kappa_{POA}$  and  $\kappa_{SOA}$  are 0.05 and 0.18, respectively. The numbers in parentheses are slopes and correlation coefficients ( $R^2$ ) of linear fits through the data. The black dashed lines are 1:1 lines.

shown in Figure 5, we conclude that changes of 15–18% in  $\kappa$  (corresponding to a change in critical diameter from 89 to 94 nm at  $S = 0.2\%$ ) will lead to about a 22% change in  $N_{CCN}$ . Increasing  $\kappa_{SOA}$  all the way to the ~upper limit of 0.3 (Petters et al., 2016) with an accompanying change in  $\kappa_{chem}$  from 0.41 to 0.426 reduces the underestimate in  $N_{CCN}$  only to 15%, indicating that underestimation of  $\kappa_{SOA}$  may explain at most 7% of the total.

For the aerosol sampled at the BJ site,  $N_{CCN}$  is overestimated by 45% at  $S = 0.2\%$  when using the BK-INT scheme, suggesting that changes of 25–30% in  $\kappa$  (corresponding to a change in critical diameter from 101 to 110 nm at  $S = 0.2\%$ ) will lead to about a 45% change in  $N_{CCN}$ . At a lower  $\kappa_{SOA}$  of 0.07,  $N_{CCN}$  is still overestimated by 33%, indicating that an overprediction of organic hygroscopicity could explain only about 12% of the overestimate of  $N_{CCN}$ . This is expected because most primary particles such as POA and soot are within the Aitken mode and are too small to contribute to  $N_{CCN}$ . The assumption of an internal mixture causes a large fraction of the POA and hydrophobic soot particles to be counted as CCN as, mathematically, they are blended with hygroscopic species and therefore leads to an overestimate of  $N_{CCN}$ . Thus, the BK-EXT scheme (externally mixed aerosol with constant composition over the full size range) is applied here (Figure 6c). By using the scheme the prediction is improved, with a reduced overestimation of 27% based on the  $f_{44}$ -derived  $\kappa_{chem}$ . The remaining bias is believed to be due to the simplified bulk chemical composition assumption. The accuracy of the estimates would improve if size-resolved chemical composition measurements were available (Asa-Awuku et al., 2011; Ervens et al., 2010). Overall,  $N_{CCN}$  is relatively insensitive to  $\kappa_{SOA}$ , which is likely due to the fact that the organic volume fraction at both sites is <70% (50.1% at BJ and 35.5% at XZ) (Chang et al., 2007; Wang et al., 2008).

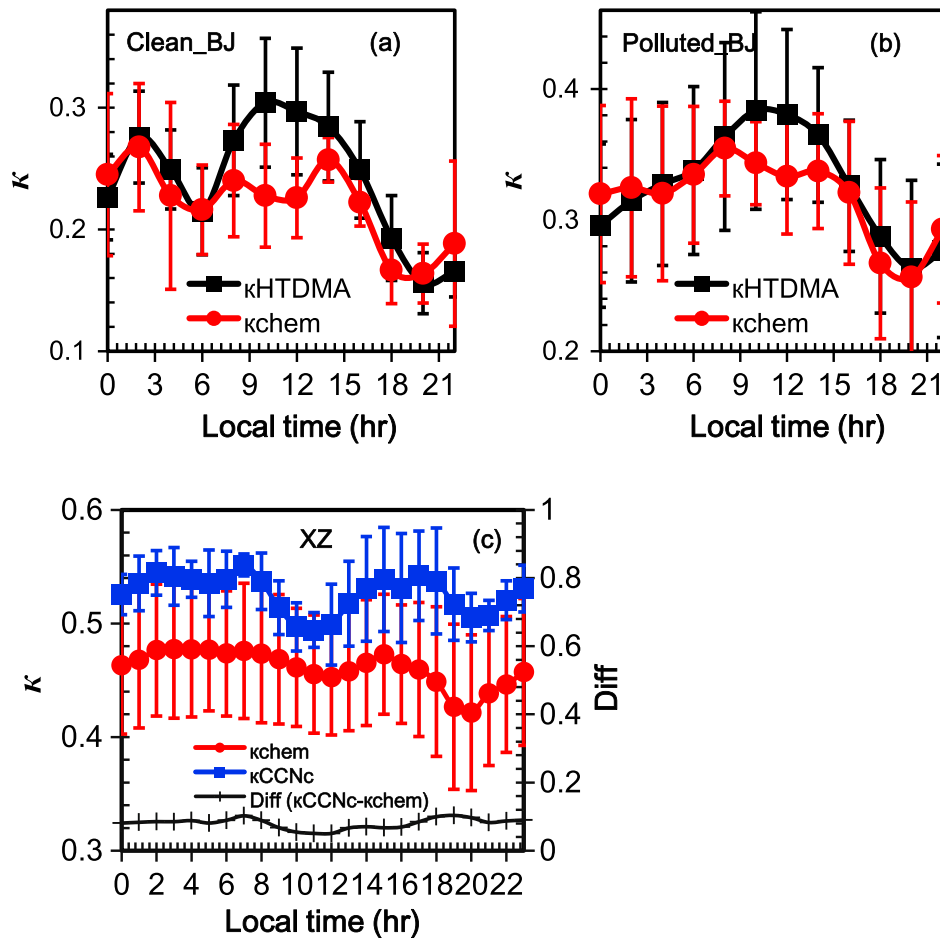


**Figure 7.** Diurnal cycles of particle hygroscopicity obtained from different measurements:  $\kappa_{HTDMA}$  and  $\kappa_{chem}$  retrieved from HTDMA and ACSM measurements, respectively, under (a) clean and (b) polluted conditions at the BJ site; (c)  $\kappa_{CCNc}$  and  $\kappa_{chem}$  retrieved from CCNc and ACSM measurements at the XZ site, and the difference between  $\kappa_{CCNc}$  and  $\kappa_{chem}$ .

Our results from BJ agree well with other studies conducted in urban areas with large contributions from freshly emitted particles (e.g., Bhattu et al., 2015; Broekhuizen et al., 2006; Cubison et al., 2008; Medina et al., 2007; Mochida et al., 2006; Quinn et al., 2008), with all reporting overestimated  $N_{CCN}$  when assuming either an internal mixing state or an external mixing state but with bulk chemical composition. The BK-INT assumption often results in an overestimate of  $N_{CCN}$ , which is inconsistent with the observed underestimation for aged aerosols measured during this study. In several studies of aged aerosols (e.g., Bougiatioti et al., 2009; Chang et al., 2007; Kuwata et al., 2008; Wang et al., 2010),  $N_{CCN}$  was also underestimated, although the authors argue that closure was achieved within acceptable errors ( $\pm 20\%$ ). Here we show a more significant underestimation of 22% at  $S = 0.2\%$ . The underestimation is even larger at lower  $S$  (not shown here); for example,  $N_{CCN}$  is underestimated by 36% at about  $S = 0.1\%$ . The underestimation of  $N_{CCN}$  corresponds to at least 7–14% in the uncertainty of derived cloud droplet number concentration (Sotiropoulou et al., 2006), and, if representative of the globe, would result in roughly a  $0.5 \text{ W m}^{-2}$  uncertainty in indirect forcing (Sotiropoulou et al., 2007).

### 3.4. Aerosol Hygroscopicity Enhanced by Atmospheric Aging/Coating Process

As described in section 3.2, the low  $\kappa_{chem}$  at XZ and the resulting underestimation of  $N_{CCN}$  it would cause is likely due to particle aging/coating processes, for example, condensation of secondary aerosol components such as sulfate and nitrate on preexisting particles. To further evaluate this hypothesis we investigate the diurnal cycles of particle hygroscopicity at BJ and XZ based on the different measurements (Figure 7). As is stated previously, because the ACSM measurements show aerosol volume was dominated by particles

with  $D_p > 60$  nm, the  $\kappa_{\text{HTDMA}}$  at BJ in Figure 7 is calculated based on measurements of particles with diameters  $>60$  nm for comparison in order to strengthen the signal due to coating effect.

From the diurnal cycles of  $\kappa_{\text{chem}}$  and  $\kappa_{\text{HTDMA}}$  in clean (Figure 7a) and polluted (Figure 7b) conditions, it is clear that  $\kappa_{\text{HTDMA}}$  peaks in the afternoon, but that no associated peaks in  $\kappa_{\text{chem}}$  are observed. This feature is stronger on clear days when atmospheric oxidation and the aging process are more rapid. Between 10:00 and 14:00 the disparity in particle hygroscopicity is from  $\sim 0.23$  ( $\kappa_{\text{chem}}$ ) to  $\sim 0.30$  ( $\kappa_{\text{HTDMA}}$ ) in clean conditions and  $\sim 0.37$  ( $\kappa_{\text{chem}}$ ) to  $\sim 0.41$  ( $\kappa_{\text{HTDMA}}$ ) on polluted days, equivalent to between 11% and 30% enhancements accompanying aging and coating of the particles. In contrast, no significant differences between  $\kappa_{\text{chem}}$  and  $\kappa_{\text{HTDMA}}$  are observed at night and in the early morning due to the lack of photochemical production of secondary hygroscopic species. Figure 7 suggests that particle hygroscopicity cannot always be accurately predicted from  $\kappa_{\text{chem}}$  calculated from the simple mixing rule in equation (4). Previous studies have shown that freshly emitted POA and BC particles may be rapidly coated by more hygroscopic components in polluted urban areas, resulting in enhanced hygroscopicity of the mixed particles (Johnson et al., 2005; Zhang et al., 2004; Zhao et al., 2017). Interestingly, such an effect was not evident in the diurnal cycles for the already well mixed aerosol present at XZ, where  $\kappa_{\text{chem}}$  and  $\kappa_{\text{HTDMA}}$  showed similar diurnal variations (Figure 7c) with a roughly constant bias between  $\kappa_{\text{CCNc}}$  and  $\kappa_{\text{chem}}$  of between 15% and 18%. This day/night contrast can be explained by the decreased rate of oxidation and condensation at night in the relatively remote area. Furthermore, because the aerosol arriving at XZ is already aged and internally mixed, the impact of additional coating is minimal. We conclude that  $N_{\text{CCN}}$  at XZ is significantly underestimated by the  $\kappa_{\text{chem}}$  model with the BK-INT assumption because the coating effect is neglected.

#### 4. Summary

Using a comprehensive data set from field measurements made at three sites in China, the prediction of particle CCN activity was evaluated. On the basis of measured size-resolved CCN activities and hygroscopic growth factors in the three distinct environments, we categorized the aerosol characteristics of BJ, XH, and XZ sites as primary, transitional, and aged, respectively. We showed a marked underestimation ( $\sim 22\%$ ) of  $N_{\text{CCN}}$  for the aged aerosol when assuming particles are internally mixed with uniform submicron chemical composition. We attributed the underestimation to neglect of the influence of particle coating and physical mixing, which was supported by the diurnal cycles of  $\kappa_{\text{chem}}$  and  $\kappa_{\text{HTDMA}}$ . Owing to the aging/coating effect, particle hygroscopicity was enhanced by between  $\sim 11\%$  (polluted conditions) and  $\sim 30\%$  (clean days). In contrast to the results obtained for the aged aerosol at XZ, for the aerosol at BJ for which freshly emitted particles contributed significantly to the total concentration the CCN activity was overestimated. That bias is likely due to the use of inaccurate assumptions of particle mixing state and of variability in composition with particle size. Our study also shows that for both aerosol types  $N_{\text{CCN, predicted}}$  exhibits very limited sensitivity to  $\kappa_{\text{SOA}}$ , which implies a critical role of other factors like mixing state and coating/aging in regulating CCN activity.

Thus, it is evident that CCN activity is linked not only to particle composition but also to mixing state and to aging and physical mixing processes (like coating and condensation), which should be elucidated and quantified through further laboratory experiments. However, our findings suggest that CCN activity of aged aerosols in northern China can approach that of pure inorganic aerosol (i.e., pure sulfate), which may also be true in other regions of the globe. Long-term observations from more ground sites, as well as aerosol data sets derived from aircraft measurements made at cloud base, should be made to better parameterize CCN.

#### Acknowledgments

This work was funded by the NSFC research project (41675141 and 91544217), the fundamental Research Funds for the Central Universities, the National Basic Research Program of China "973" (2013CB955804), and the NSCF-TAMU Collaborative Research Grant Program (4141101031), and the Natural Science Foundation (NSF) (AGS1534670). We thank all participants in the field campaigns for their tireless work and cooperation. The data used for this paper are available on request to the corresponding author.

#### References

- Andreae, M. O. (2009). Correlation between cloud condensation nuclei concentration and aerosol optical thickness in remote and polluted regions. *Atmospheric Chemistry and Physics*, 9, 543–556.
- Asa-Awuku, A., Moore, R. H., Nenes, A., Bahreini, R., Holloway, J. S., Brock, C. A., ... Huey, L. G. (2011). Airborne cloud condensation nuclei measurements during the 2006 Texas air quality study. *Journal of Geophysical Research*, 116, D11201. <https://doi.org/10.1029/2010JD014874>
- Bhattu, D., & Tripathi, S. N. (2015). CCN closure study: Effects of aerosol chemical composition and mixing state. *Journal of Geophysical Research: Atmospheres*, 120, 766–783. <https://doi.org/10.1002/2014JD021978>
- Bougiatioti, A., Fountoukis, C., Kalivitis, N., Pandis, S. N., Nenes, A., & Mihalopoulos, N. (2009). Cloud condensation nuclei measurements in the marine boundary layer of the Eastern Mediterranean: CCN closure and droplet growth kinetics. *Atmospheric Chemistry and Physics*, 9, 7053–7066. <https://doi.org/10.5194/acp-9-7053-2009>

- Bougiatioti, A., Nenes, A., Fountoukis, C., Kalivitis, N., Pandis, S. N., & Mihalopoulos, N. (2011). Size-resolved CCN distributions and activation kinetics of aged continental and marine aerosol. *Atmospheric Chemistry and Physics*, 11, 8791–8808. <https://doi.org/10.5194/acp-11-8791-2011>
- Broekhuizen, K., Chang, R. Y. W., Leaitch, W. R., Li, S. M., & Abbatt, J. P. D. (2006). Closure between measured and modeled cloud condensation nuclei (CCN) using size-resolved aerosol compositions in downtown Toronto. *Atmospheric Chemistry and Physics*, 6, 2513–2524. <https://doi.org/10.5194/acp-6-2513-2006>
- Cerully, K. M., Raatikainen, T., Lance, S., Tkacik, D., Tiitta, P., Petäjä, T., ... Nenes, A. (2011). Aerosol hygroscopicity and CCN activation kinetics in a boreal forest environment during the 2007 EUCAARI campaign. *Atmospheric Chemistry and Physics*, 11, 12,369–12,386. <https://doi.org/10.5194/acp-11-12369-2011>
- Chang, R. W., Liu, P. S. K., Leaitch, W. R., & Abbatt, J. P. D. (2007). Comparison between measured and predicted CCN concentrations at Egbert, Ontario: Focus on the organic aerosol fraction at a semi-rural site. *Atmospheric Environment*, 41(37), 8172–8182.
- Chuang, P. Y., Collins, D. R., Pawlowska, H., Snider, J. R., Jonsson, H. H., Brenguier, J. L., ... Seinfeld, J. H. (2000). CCN measurements during ACE-2 and their relationship to cloud microphysical properties. *Tellus B*, 52, 843–867.
- Clegg, S. L., Brimblecombe, P., & Wexler, A. S. (1998). Thermodynamic model of the system  $\text{H}^+ - \text{NH}_4^+ - \text{Na}^+ - \text{SO}_4^{2-} - \text{NH}_3 - \text{Cl}^- - \text{H}_2\text{O}$  at 298.15 K. *The Journal of Physical Chemistry A*, 102(12), 2155–2171.
- Collins, D. R., Flagan, R. C., & Seinfeld, J. H. (2002). Improved inversion of scanning DMA data. *Aerosol Science and Technology*, 36, 1–9.
- Cruz, C. N., & Pandis, S. N. (1997). A study of the ability of pure secondary organic aerosol to act as cloud condensation nuclei. *Atmospheric Environment*, 31, 2205–2214. [https://doi.org/10.1016/S1352-2310\(97\)00054-X](https://doi.org/10.1016/S1352-2310(97)00054-X)
- Cubison, M. J., Ervens, B., Feingold, G., Docherty, K. S., Ulbrich, I. M., Shields, L., ... Jimenez, J. L. (2008). The influence of chemical composition and mixing state of Los Angeles urban aerosol on CCN number and cloud properties. *Atmospheric Chemistry and Physics*, 8, 5649–5667. <https://doi.org/10.5194/acp-8-5649-2008>
- Deng, Z., Zhao, C., Ma, N., Liu, F., Ran, L., Xu, W., ... Yan, P. (2011). Size-resolved and bulk activation properties of aerosols in the North China Plain. *Atmospheric Chemistry and Physics*, 11, 3835–3846.
- Dusek, U., Frank, G. P., Hildebrandt, L., Curtius, J., Schneider, J., Walter, S., ... Andreae, M. O. (2006). Size matters more than chemistry for cloud-nucleating ability of aerosol particles. *Science*, 312, 1375–1378.
- Ervens, B., Cubison, M. J., Andrews, E., Feingold, G., Ogren, J. A., Jimenez, J. L., ... Allan, J. D. (2010). CCN predictions using simplified assumptions of organic aerosol composition and mixing state: A synthesis from six different locations. *Atmospheric Chemistry and Physics*, 10(10), 4795–4807.
- Farmer, D. K., Cappa, C. D., & Kreidenweis, S. M. (2015). Atmospheric processes and their controlling influence on cloud condensation nuclei activity. *Chemical Reviews*, 115(10), 4199–4217.
- Gasparini, R., Collins, D. R., Andrews, E., Sheridan, P. J., Ogren, J. A., & Hudson, J. G. (2006). Coupling aerosol size distributions and size-resolved hygroscopicity to predict humidity-dependent optical properties and cloud condensation nuclei spectra. *Journal of Geophysical Research*, 111, D05S13. <https://doi.org/10.1029/2005JD006092>
- Gasparini, R., Li, R., & Collins, D. R. (2004). Integration of size distributions and size-resolved hygroscopicity measured during the Houston Supersite for compositional categorization of the aerosol. *Atmospheric Environment*, 38, 3285–3303.
- Ghan, S. J., Rissman, T. A., Elleman, R., Ferrare, R. A., Turner, D., Flynn, C., ... Seinfeld, J. H. (2006). Use of in situ cloud condensation nuclei, extinction, and aerosol size distribution measurements to test a method for retrieving cloud condensation nuclei profiles from surface measurements. *Journal of Geophysical Research*, 111, D05S10. <https://doi.org/10.1029/2004JD005752>
- Good, N., Topping, D. O., Allan, J. D., Flynn, M., Fuentes, E., Irwin, M., ... McFiggans, G. (2010). Consistency between parameterisations of aerosol hygroscopicity and CCN activity during the RHaMBLe discovery cruise. *Atmospheric Chemistry and Physics*, 10, 3189–3203. <https://doi.org/10.5194/acp-10-3189-2010>
- Irwin, M., Good, N., Crosier, J., Choulaton, T. W., & McFiggans, G. (2010). Reconciliation of measurements of hygroscopic growth and critical supersaturation of aerosol particles in central Germany. *Atmospheric Chemistry and Physics*, 10, 11,737–11,752. <https://doi.org/10.5194/acp-10-11737-2010>
- Jiang, R. X., Tan, H. B., Tang, L. L., Cai, M. F., Yin, Y., Li, F., ... Wu, D. (2016). Comparison of aerosol hygroscopicity and mixing state between winter and summer seasons in Pearl River Delta region, China. *Atmospheric Research*, 169, 160–170.
- Jimenez, J. L., Canagaratna, M. R., Donahue, N. M., Prevot, A. S. H., Zhang, Q., Kroll, J. H., ... Worsnop, D. R. (2009). Evolution of organic aerosols in the atmosphere. *Science*, 326, 1525–1529. <https://doi.org/10.1126/science.1180353>
- Johnson, K. S., Zuberi, B., Molina, L. T., Molina, M. J., Iedema, M. J., Cowin, J. P., ... Laskin, A. (2005). Processing of soot in an urban environment: Case study from the Mexico City Metropolitan Area. *Atmospheric Chemistry and Physics*, 5, 3033–3043. <https://doi.org/10.5194/acp-5-3033-2005>
- Juranyi, Z., Gysel, M., Weingartner, E., DeCarlo, P. F., Kammermann, L., & Baltensperger, U. (2010). Measured and modelled cloud condensation nuclei number concentration at the high alpine site Jungfraujoch. *Atmospheric Chemistry and Physics*, 10, 7891–7906.
- Koehler, H. (1936). The nucleus in and growth of hygroscopic droplets. *Transactions of the Faraday Society*, 32, 1152–1161. <https://doi.org/10.1039/TF9363201152>
- Kuwata, M., Kondo, Y., Miyazaki, Y., Komazaki, Y., Kim, J. H., Yum, S. S., ... Matsueda, H. (2008). Cloud condensation nuclei activity at Jeju Island, Korea in spring 2005. *Atmospheric Chemistry and Physics*, 8, 2933–2948. <https://doi.org/10.5194/acp-8-2933-2008>
- Lance, S., Medina, J., Smith, J., & Nenes, A. (2006). Mapping the operation of the DMT continuous flow CCN counter. *Aerosol Science and Technology*, 40, 242–254.
- Liu, J., & Li, Z. (2014). Estimation of cloud condensation nuclei concentration from aerosol optical quantities: Influential factors and uncertainties. *Atmospheric Chemistry and Physics*, 14(1), 471–483.
- Liu, P. F., Zhao, C. S., Bel, T. G., Hallbauer, E., Nowak, A., Ran, L., ... Wiedensohler, A. (2011). Hygroscopic properties of aerosol particles at high relative humidity and their diurnal variations in the North China Plain. *Atmospheric Chemistry and Physics*, 11, 2991–3040.
- Ma, Y., Brooks, S. D., Vidaurre, G., Khalizov, A. F., Wang, L., & Zhang, R. (2013). Rapid modification of cloud-nucleating ability of aerosols by biogenic emissions. *Geophysical Research Letters*, 40, 6293–6297. <https://doi.org/10.1002/2013GL057895>
- Massling, A., Leinert, S., Wiedensohler, A., & Covert, D. (2007). Hygroscopic growth of sub-micrometer and one-micrometer aerosol particles measured during ACE-Asia. *Atmospheric Chemistry and Physics*, 7, 3249–3259.
- Massling, A., Wiedensohler, A., Busch, B., Neususs, C., Quinn, P., Bates, T., & Covert, D. (2003). Hygroscopic properties of different aerosol types over the Atlantic and Indian Oceans. *Atmospheric Chemistry and Physics*, 3, 1377–1397. <https://doi.org/10.5194/acp-3-1377-2003>
- McFiggans, G., Artaxo, P., Baltensperger, U., Coe, H., Facchini, M. C., Feingold, G., ... Weingartner, E. (2006). The effect of physical and chemical aerosol properties on warm cloud droplet activation. *Atmospheric Chemistry and Physics*, 6, 2593–2649. <https://doi.org/10.5194/acp-6-2593-2006>

- Mei, F., Hayes, P. L., Ortega, A. M., Taylor, J. W., Allan, J. D., Gilman, J. B., ... Wang, J. (2013). Droplet activation properties of organic aerosols observed at an urban site during CalNex-LA. *Journal of Geophysical Research: Atmospheres*, *118*, 2903–2917. <https://doi.org/10.1002/jgrd.50285>
- Mochida, M., Kuwata, M., Miyakawa, T., Takegawa, N., Kawamura, K., & Kondo, Y. (2006). Relationship between hygroscopicity and cloud condensation nuclei activity for urban aerosols in Tokyo. *Journal of Geophysical Research*, *111*, D23204. <https://doi.org/10.1029/2005JD006980>
- Ng, N. L., Herndon, S. C., Trimborn, A., Canagaratna, M. R., Croteau, P. L., Onasch, T. B., ... Jayne, J. T. (2011). An Aerosol Chemical Speciation Monitor (ACSM) for routine monitoring of the composition and mass concentrations of ambient aerosol. *Aerosol Science and Technology*, *45*, 770–784.
- Paatero, P., & Tapper, U. (1994). Positive matrix factorization: A nonfactor model with optimal utilization of error estimates of data values. *Environmetrics*, *5*, 111–126.
- Padro, L. T., Asa-Awuku, A., Morrison, R., & Nenes, A. (2007). Inferring thermodynamic properties from CCN activation experiments: Single-component and binary aerosols. *Atmospheric Chemistry and Physics*, *7*, 5263–5274. <https://doi.org/10.5194/acp-7-5263-2007>
- Padro, L. T., Moore, R. H., Zhang, X., Rastogi, N., Weber, R. J., & Nenes, A. (2012). Mixing state and compositional effects on CCN activity and droplet growth kinetics of size-resolved CCN in an urban environment. *Atmospheric Chemistry and Physics*, *12*(21), 10,239–10,255.
- Petters, M. D., & Kreidenweis, S. M. (2007). A single parameter representation of hygroscopic growth and cloud condensation nucleus activity. *Atmospheric Chemistry and Physics*, *7*, 1961–1971. <https://doi.org/10.5194/acp-7-1961-2007>
- Petters, M. D., Kreidenweis, S. M., & Ziemann, P. J. (2016). Prediction of cloud condensation nuclei activity for organic compounds using functional group contribution methods. *Geoscientific Model Development*, *9*(1), 111–124.
- Pradeep Kumar, P., Broekhuizen, K., & Abbatt, J. P. D. (2003). Organic acids as cloud condensation nuclei: Laboratory studies of highly soluble and insoluble species. *Atmospheric Chemistry and Physics*, *3*, 509–520. <https://doi.org/10.5194/acp-3-509-2003>
- Prenni, A. J., Petters, M. D., Kreidenweis, S. M., DeMott, P. J., & Ziemann, P. J. (2007). Cloud droplet activation of secondary organic aerosol. *Journal of Geophysical Research*, *112*, D10223. <https://doi.org/10.1029/2006JD007963>
- Pruppacher, H. R., & Klett, J. D. (2000). *Microphysics of clouds and precipitation*. Dordrecht, Netherlands: Kluwer Academic Publishers.
- Quinn, P. K., Bates, T. S., Coffman, D. J., & Covert, D. S. (2008). Influence of particle size and chemistry on the cloud nucleating properties of aerosols. *Atmospheric Chemistry and Physics*, *8*, 1029–1042. <https://doi.org/10.5194/acp-8-1029-2008>
- Rose, D., Gunthe, S. S., Mikhailov, E., Frank, G. P., Dusek, U., Andreae, M. O., & Pöschl, U. (2008). Calibration and measurement uncertainties of a continuous-flow cloud condensation nuclei counter (DMT-CCNC): CCN activation of ammonium sulfate and sodium chloride aerosol particles in theory and experiment. *Atmospheric Chemistry and Physics*, *8*, 1153–1179. <http://www.atmos-chem-phys.net/8/1153/2008/>
- Seinfeld, J. H., Bretherton, C., Carslaw, K. S., Coe, H., DeMott, P. J., Dunlea, E. J., ... Kraucunas, I. (2016). Improving our fundamental understanding of the role of aerosol–cloud interactions in the climate system. *Proceedings of the National Academy of Sciences of the United States of America*, *113*(21), 5781–5790.
- Sotiropoulou, R. E. P., Medina, J., & Nenes, A. (2006). CCN predictions: Is theory sufficient for assessments of the indirect effect? *Geophysical Research Letters*, *33*, L05816. <https://doi.org/10.1029/2005GL025148>
- Sotiropoulou, R. E. P., Nenes, A., Adams, P. J., & Seinfeld, J. H. (2007). Cloud condensation nuclei prediction error from application of Köhler theory: Importance for the aerosol indirect effect. *Journal of Geophysical Research*, *112*, D12202. <https://doi.org/10.1029/2006JD007834>
- Sun, Y., Wang, Z., Dong, H., Yang, T., Li, J., Pan, X., ... Jayne, J. T. (2012). Characterization of summer organic and inorganic aerosols in Beijing, China with an aerosol chemical speciation monitor. *Atmospheric Environment*, *51*, 250–259. <https://doi.org/10.1016/j.atmosenv.2012.01.013>
- Sun, Y. L., Wang, Z. F., Du, W., Zhang, Q., Wang, Q. Q., Fu, P. Q., ... Worsnop, D. R. (2015). Long-term real-time measurements of aerosol particle composition in Beijing, China: Seasonal variations, meteorological effects, and source analysis. *Atmospheric Chemistry and Physics*, *15*, 10,149–10,165. <https://doi.org/10.5194/acp-15-10149-2015>
- Tan, H., Xu, H., Wan, Q., Li, F., Deng, X., Chan, P. W., ... Yin, Y. (2013). Design and application of an unattended multifunctional H-TDMA system. *Journal of Atmospheric and Oceanic Technology*, *30*(6), 1136–1148.
- Turpin, B. J., & Lim, H. J. (2001). Species contributions to PM<sub>2.5</sub> mass concentrations: Revisiting common assumptions for estimating organic mass. *Aerosol Science and Technology*, *35*(1), 602–610.
- Ulbrich, I. M., Canagaratna, M. R., Zhang, Q., Worsnop, D. R., & Jimenez, J. L. (2009). Interpretation of organic components from Positive Matrix Factorization of aerosol mass spectrometric data. *Atmospheric Chemistry and Physics*, *9*, 2891–2918. <https://doi.org/10.5194/acp-9-2891-2009>
- Vu, D., Short, D., Karavalakis, G., Durbin, T. D., & Asa-Awuku, A. (2017). Will aerosol hygroscopicity change with biodiesel, renewable diesel fuels and emission control technologies? *Environmental Science & Technology*, *51*(3), 1580.
- Wang, J., Cubison, M. J., Aiken, A. C., Jimenez, J. L., & Collins, D. R. (2010). The importance of aerosol mixing state and size-resolved composition on CCN concentration and the variation of the importance with atmospheric aging of aerosols. *Atmospheric Chemistry and Physics*, *10*(15), 7267–7283.
- Wang, S. C., & Flagan, R. C. (1990). Scanning electrical mobility spectrometer. *Aerosol Science and Technology*, *13*, 230–240.
- Wang, J., Lee, Y. N., Daum, P. H., Jayne, J., & Alexander, M. L. (2008). Effects of aerosol organics on cloud condensation nucleus (CCN) concentration and first indirect aerosol effect. *Atmospheric Chemistry and Physics*, *8*(21), 6325–6339.
- Wang, Y., Zhang, F., Li, Z., Tan, H., Xu, H., Ren, J., ... Sun, Y. (2017). Enhanced hydrophobicity and volatility of submicron aerosols under severe emission control conditions in Beijing. *Atmospheric Chemistry and Physics*, *17*, 5239–5251. <https://doi.org/10.5194/acp-17-5239-2017>
- Wang, Q., Zhao, J., Du, W., Ana, G., Wang, Z., Sun, L., ... Sun, Y. (2016). Characterization of submicron aerosols at a suburban site in central China. *Atmospheric Environment*, *131*, 115–123.
- Wex, H., Petters, M. D., Carrico, C. M., Hallbauer, E., Massling, A., McMeeking, G. R., ... Stratmann, F. (2009). Towards closing the gap between hygroscopic growth and activation for secondary organic aerosol: Part 1—Evidence from measurements. *Atmospheric Chemistry and Physics*, *9*, 3987–3997. <https://doi.org/10.5194/acp-9-3987-2009>
- Wiedensohler, A. (1988). An approximation of the bipolar charge distribution for particles in the submicron size range. *Journal of Aerosol Science*, *19*, 387–389.
- Wiedensohler, A., Birmili, W., Nowak, A., Sonntag, A., Weinhold, K., Merkel, M., ... Bastian, S. (2012). Mobility particle size spectrometers: Harmonization of technical standards and data structure to facilitate high quality long-term observations of atmospheric particle number size distributions. *Atmospheric Measurement Techniques*, *5*, 657–685. <https://doi.org/10.5194/amt-5-657-2012>
- Wu, Z. J., Poulain, L., Henning, S., Dieckmann, K., Birmili, W., Merkel, M., ... Wiedensohler, A. (2013). Relating particle hygroscopicity and CCN activity to chemical composition during the HCCT-2010 field campaign. *Atmospheric Chemistry and Physics*, *13*, 7983–7996. <https://doi.org/10.5194/acp-13-7983-2013>

- Wu, Z. J., Zheng, J., Shang, D. J., Du, Z. F., Wu, Y. S., Zeng, L. M., & Hu, M. (2016). Particle hygroscopicity and its link to chemical composition in the urban atmosphere of Beijing, China, during summertime. *Atmospheric Chemistry and Physics*, *16*(2), 1123–1138.
- Ye, X., Tang, C., Yin, Z., Chen, J., Ma, Z., Kong, L., ... Geng, F. (2013). Hygroscopic growth of urban aerosol particles during the 2009 Mirage-Shanghai Campaign. *Atmospheric Environment*, *64*, 263–269. <https://doi.org/10.1016/j.atmosenv.2012.09.064>
- Zhang, F., Li, Z., Li, Y., Sun, Y., Wang, Z., Li, P., ... Wang, Q. (2016). Impacts of organic aerosols and its oxidation level on CCN activity from measurement at a suburban site in China. *Atmospheric Chemistry and Physics*, *16*(8), 5413–5425.
- Zhang, F., Li, Z., Li, R. J., Sun, L., Zhao, C., Wang, P. C., ... Fan, T. Y. (2014). Aerosol hygroscopicity and cloud condensation nuclei activity during the AC3Exp campaign: Implications for cloud condensation nuclei parameterization. *Atmospheric Chemistry and Physics*, *14*, 13,423–13,437.
- Zhang, S. L., Ma, N., Kecorius, S., Wang, P. C., Hu, M., Wang, Z. B., ... Wiedensohler, A. (2016). Mixing state of atmospheric particles over the North China Plain. *Atmospheric Environment*, *125*, 152–164. <https://doi.org/10.1016/j.atmosenv.2015.10.053>
- Zhang, Q., Stanier, C. O., Canagaratna, M. R., Jayne, J. T., Worsnop, D. R., Pandis, S. N., & Jimenez, J. L. (2004). Insights into the chemistry of new particle formation and growth events in Pittsburgh based on aerosol mass spectrometry. *Environmental Science & Technology*, *38*(18), 4797–4809. <https://doi.org/10.1021/es035417u>
- Zhao, J., Du, W., Zhang, Y., Wang, Q., Chen, C., Xu, W., & Li, Z. (2017). Insights into aerosol chemistry during the 2015 China Victory Day parade: Results from simultaneous measurements at ground level and 260 m in Beijing. *Atmospheric Chemistry and Physics*, *17*(4), 3215–3232.